

PP and PS imaging and reflectivity of the Ardley coal zone, Red Deer, Alberta

Sarah E. Richardson and Don C. Lawton

SUMMARY

Walkway VSP surveys obtained of coal strata near Red Deer demonstrate good quality compressional and converted-wave imaging of the coal zone. Reflectivity analysis of the top of coal reflection demonstrates that PP reflectivity values differ substantially from those predicted by single-interface numerical modelling. Detailed numerical modelling, including several interfaces within the coal zone as well as the base of coal reflection yields predicted reflectivity values much nearer those extracted from field data, and result from thin-bed tuning. PS reflectivity values, however, match those predicted by single-interface numerical modelling well, indicating that they are less affected by tuning effects than the PP reflectivity values.

INTRODUCTION

Zero-offset vertical seismic profiles (VSPs), multioffset (“walkaway”) VSPs, and surface seismic were acquired at the Cygnet 9-34-38-28W4 lease site near Red Deer. Suncor Energy Inc., industry partners, and the Alberta Research Council are evaluating this site for enhanced coalbed methane recovery. Methane production and carbon dioxide sequestration are both being tested for viability within the lower Tertiary Ardley

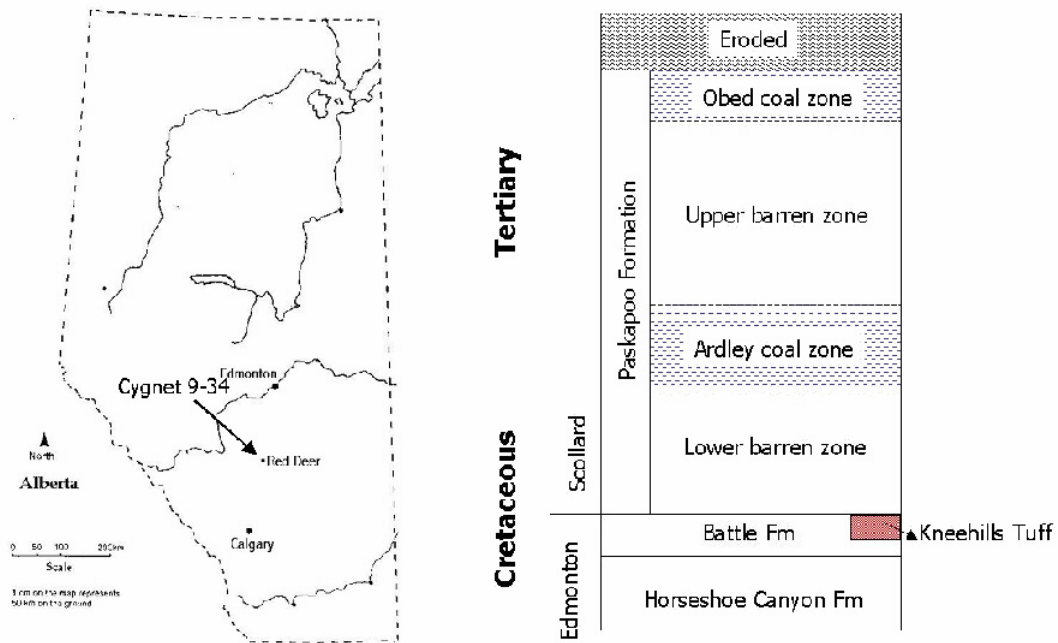


FIG.1. Location and stratigraphy of the Red Deer coalbed methane test site (Natural Resources Canada, 2002, and Gibson, 1977).

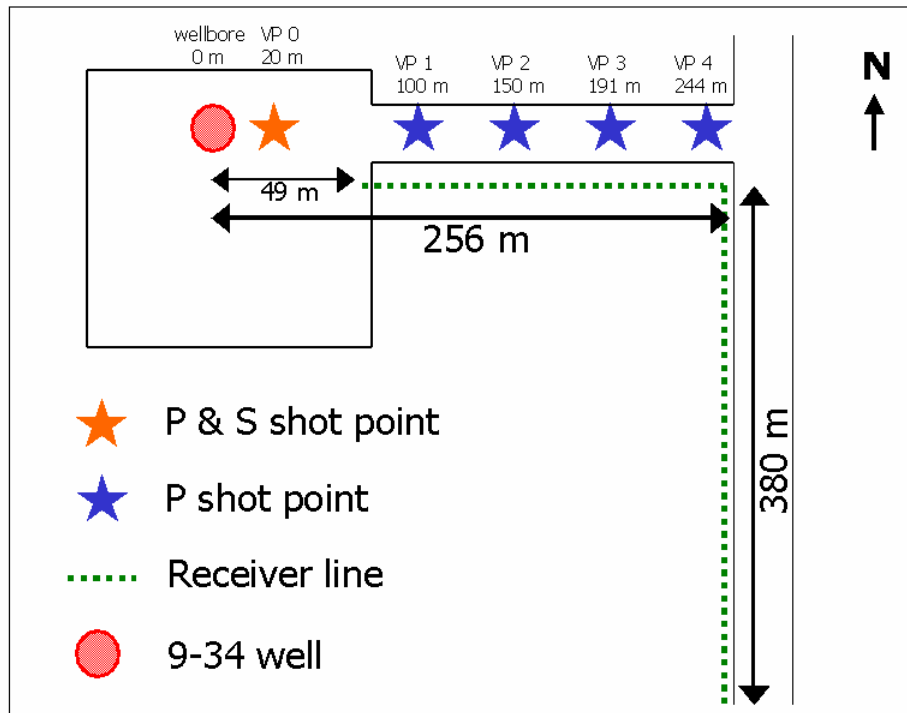


FIG. 2. Plan view geometry of acquisition at 9-34-38-28W4 near Red Deer. Walkaway source points were located at VP1 to VP4. Surface receivers were spaced at 10 m increments, illustrated by the green dashed line.

coal zone (Figure 1), one of Alberta's most prospective CBM targets. The Ardley coals are at a depth of 282 m below surface at this location. The geometry for all surveys is illustrated in Figure 2.

Multioffset surveys were conducted using a truck-mounted "mini" Vibroseis P-wave source, sweeping 8-250 Hz with a 1 ms sampling rate. Four shot points East of the borehole were used for these surveys, at offsets of 99 m, 150 m, 191 m, and 244 m from the borehole. For these walkaway surveys, three-component receivers were located at 15 m intervals from TD to surface of the wellbore.

Single vertical-component surface seismic data were recorded during the shooting of the vertical seismic profiles, using a 60-channel Geometrics 'Strataview' seismic recorder. Geophones were spread at 10 m intervals East along the lease road and South along the Range road as illustrated in Figure 2.3. Surface data were also recorded, using the zero-offset VSP shots (both mini-P and big-P) as sources, as well as the walkaway shots.

WALKAWAY VSP DATA

Processing of the walkaway VSP data set was performed by Schlumberger Canada. Separated upgoing and downgoing P and S wavefields show relatively noise-free data (Figures 3-6).

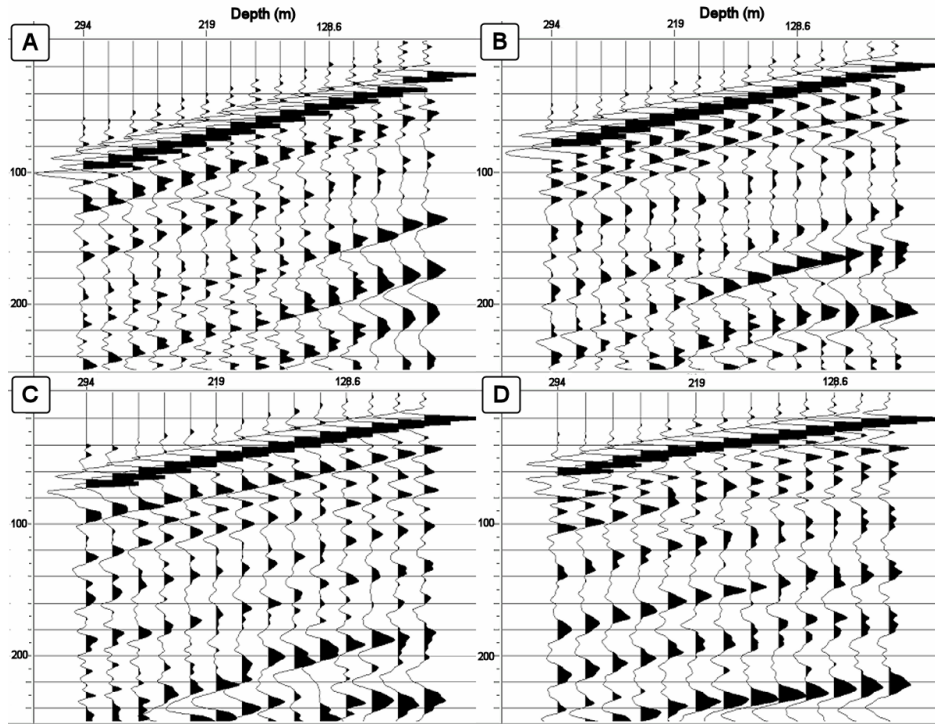


FIG. 3. Downgoing P-wavefields for source offsets of: A) 100 m, B) 150 m, C) 191 m, D) 244 m. Receivers are ordered from deepest to shallowest (left to right). All time scales are in milliseconds.

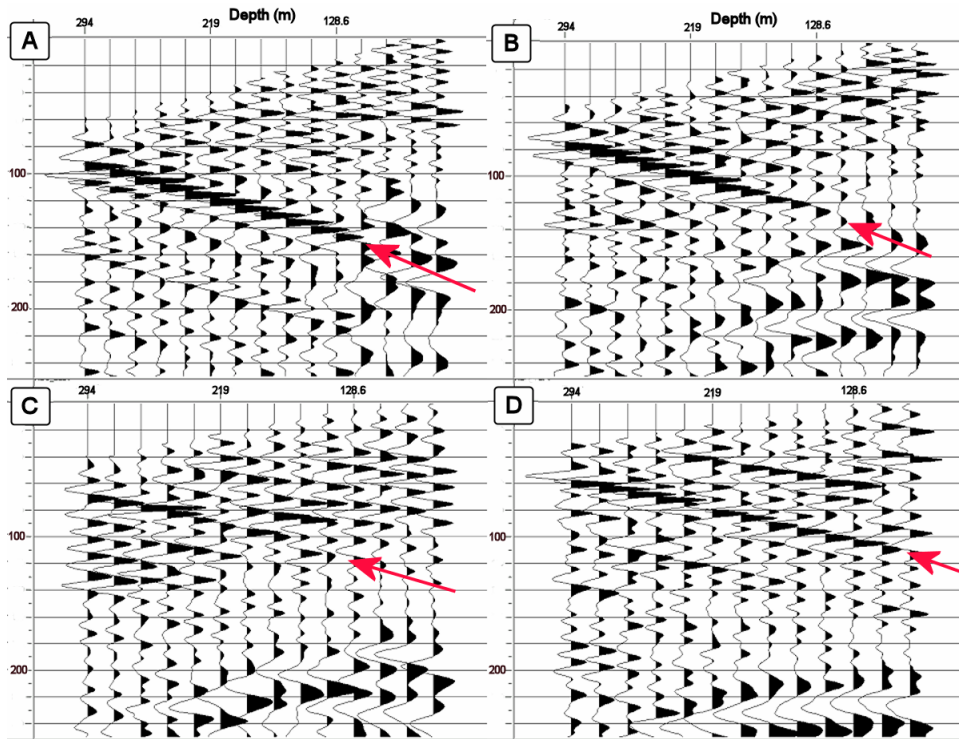


FIG. 4. Upgoing P-wavefields for source offsets of: A) 100 m, B) 150 m, C) 191 m, D) 244 m. Receivers are ordered from deepest to shallowest (left to right). Upgoing energy is indicated with an arrow.

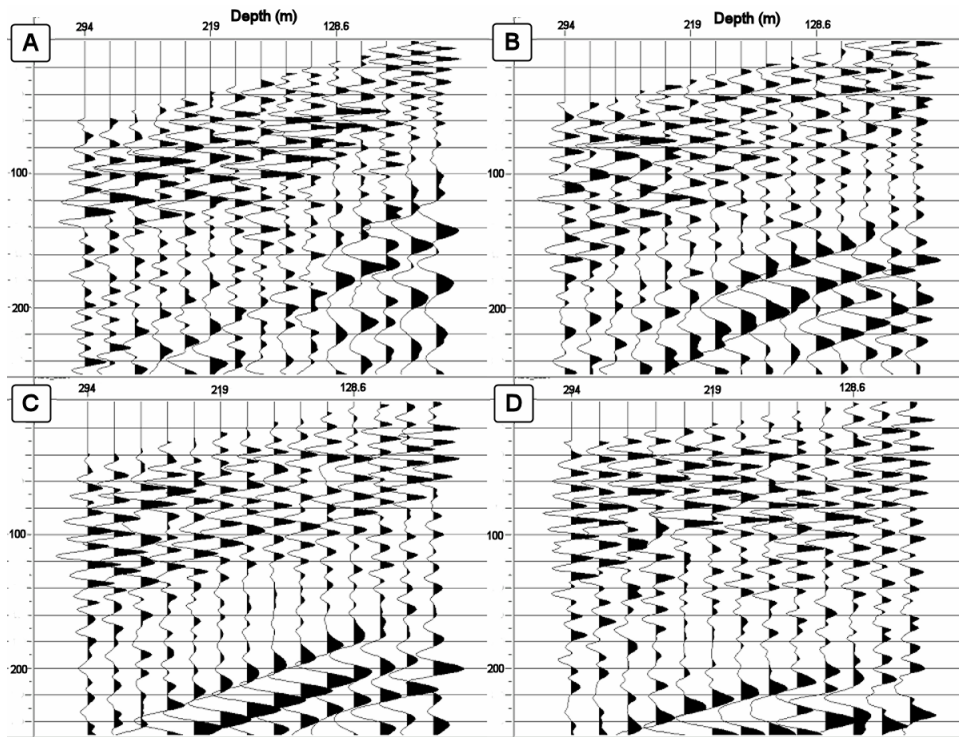


FIG. 5. Downgoing S-wavefields for source offsets of: A) 100 m, B) 150 m, C) 191 m, D) 244 m. Receivers are ordered from deepest to shallowest (left to right).

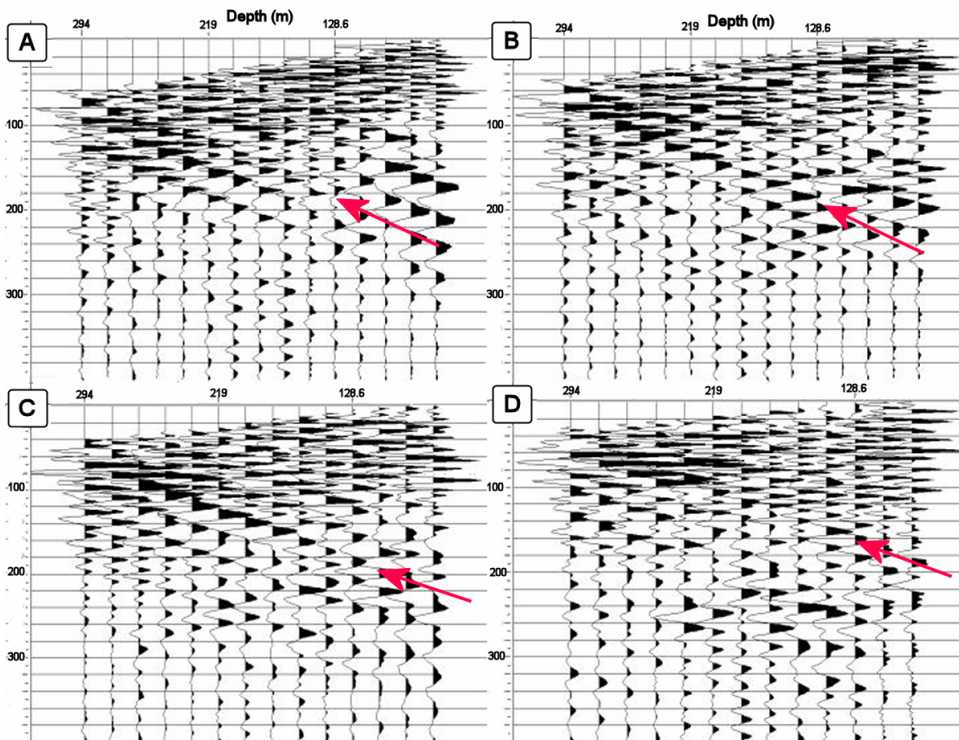


FIG. 6. Upgoing S-wavefields for source offsets of: A) 100 m, B) 150 m, C) 191 m, D) 244 m. Receivers are ordered from deepest to shallowest (left to right). Upgoing energy is highlighted with an arrow.

These separated wavefields were further processed to produce the final VSP-CDP stack for P-P data and VSP-CCP stack for P-S reflections. Both CDP and CCP mapping show good correlation with the zero-offset corridor stacks and with synthetic seismograms (Figure 7 and Figure 8, respectively). Events are aligned in time, and relative amplitudes are similar throughout the sections. Coal contacts are clearly resolved across the section in both the compressional and converted-wave data.

VSP-CDP mapping correlates well with zero-offset data, demonstrating slightly lower bandwidth. At the nearest offset (100 m), the converted-wave data shows even more detail at the coal top, showing a double-trough event, whereas the P-P data shows a single trough representing the coal top. At the furthest offset (244 m), the compressional data gives a more continuous coal response than the converted wave imaging. At the level of the coal top, the VSP-CCP gather at 244 m source offset shows an apparent phase change. Without another source offset, it is not possible to tell whether this is a processing artifact or a legitimate phase change, but variations in reflections both above and below the coal top in this gather suggest that it is the result of processing. Additionally, no phase change is noted on the offset synthetic seismogram.

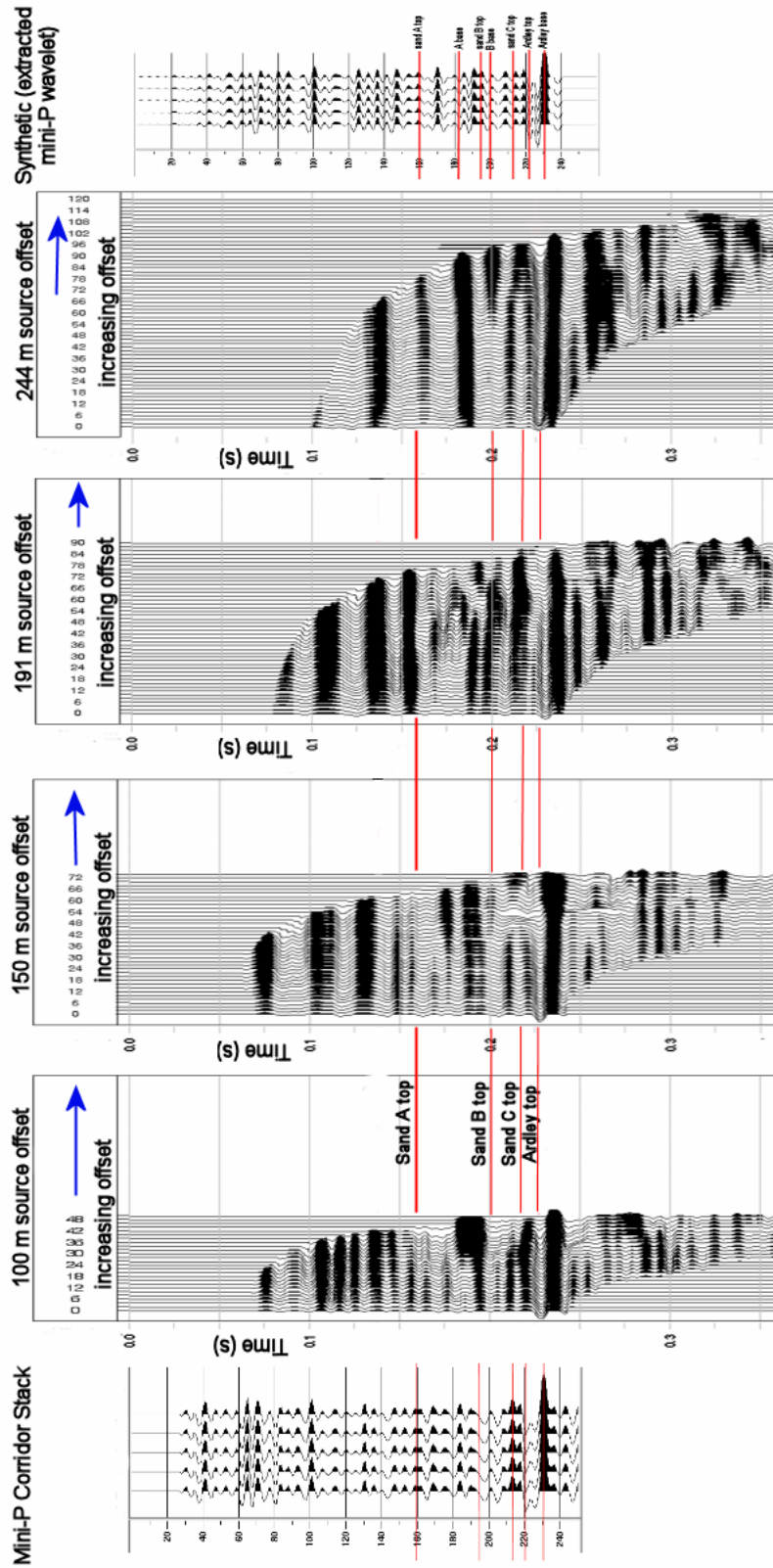


FIG. 7. Comparison of VSP-CDP mapping with mini-P zero-offset corridor stack and synthetic seismogram created by convolution with extracted mini-P wavelet. All events correlate well, although higher bandwidth is evident in the zero-offset corridor stack.

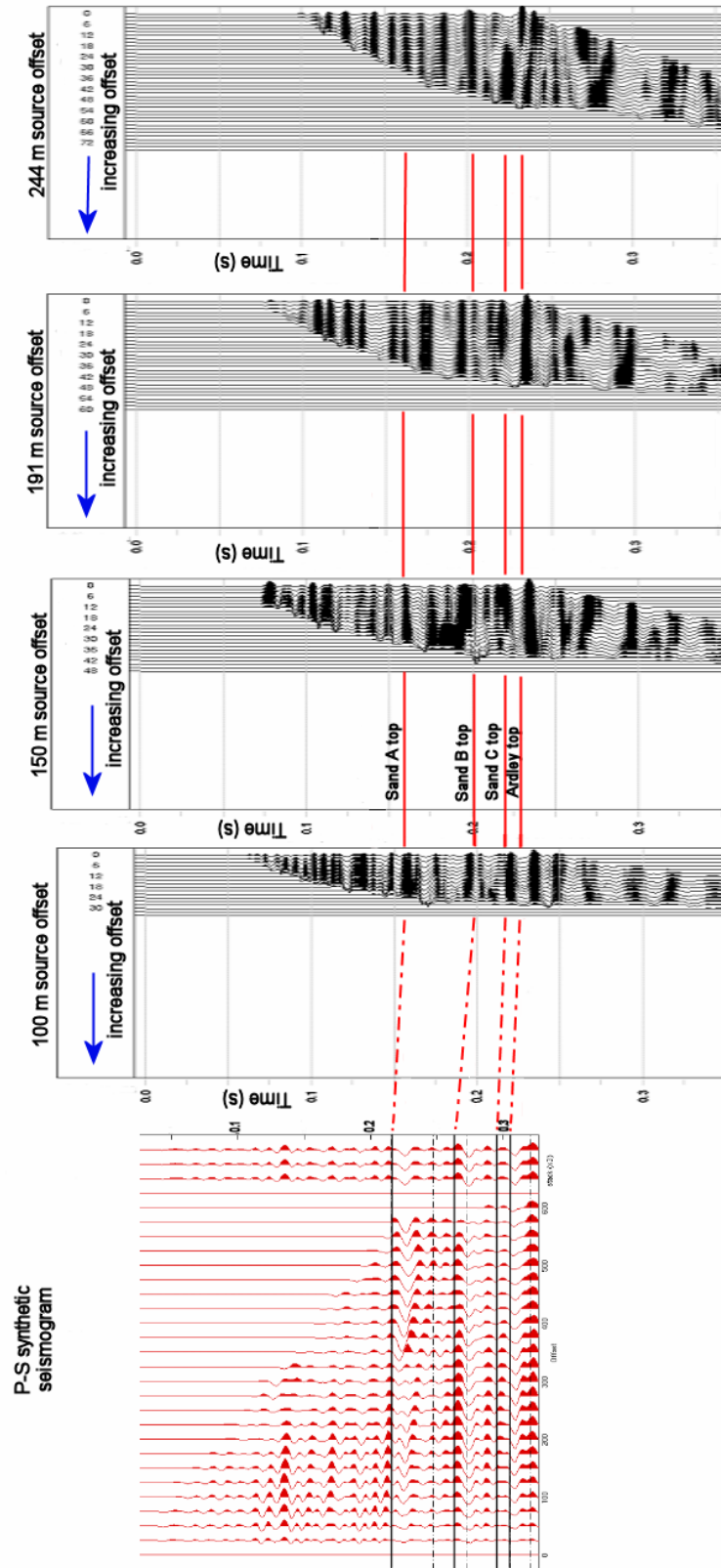


FIG. 8. Comparison of VSP-CCP transform with P-S synthetic seismogram. VSP-CCP transforms are plotted in P-time.

SURFACE SEISMIC DATA

Processing of the surface seismic data proved to be limited as a result of the unusual acquisition geometry (Figure 2). A simple processing flow was applied to the raw shot records, however, such that coal reflections may be assessed on surface seismic data. A sample shot record is illustrated in Figure 9. The surface data does not tie perfectly with the big-P corridor stack, time-wise.

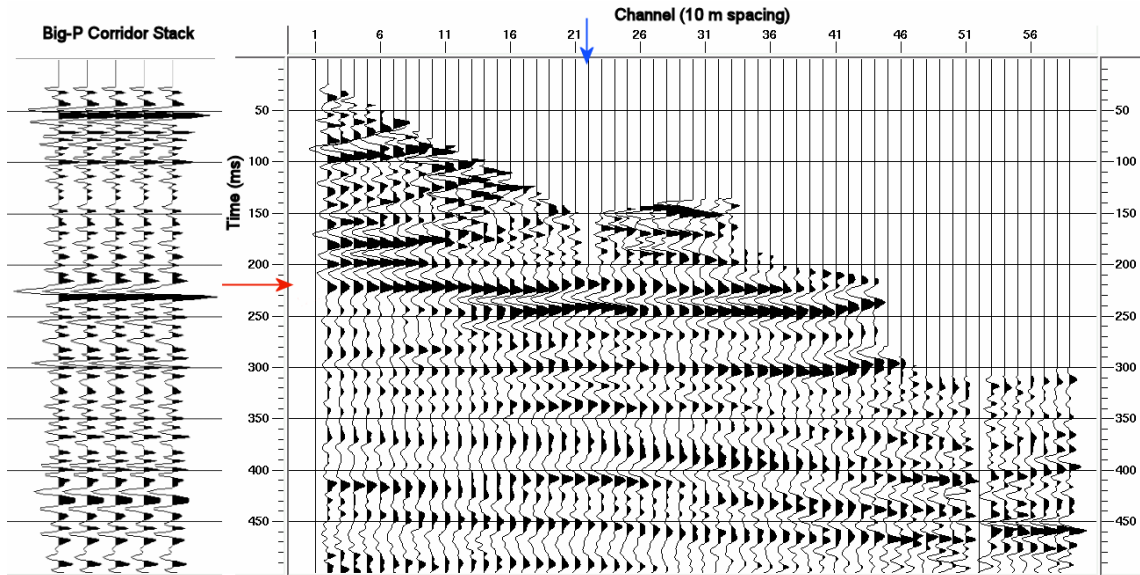


FIG. 9. Shot record from surface seismic data recorded at Red Deer. Receiver number 22 (highlighted by blue arrow) indicates the location of the corner in the L-shaped receiver line.

The time of the big-P upper coal reflection (as indicated by the red arrow) does not tie with the coal reflection imaged in the surface seismic data, but strong coal events are indeed noted on the shot record, slightly later than those imaged using the VSP. The strength of the coal response recorded on the surface data suggests that a mini-P Vibroseis is a suitable source for not only VSP data, but also surface surveys imaging Ardley coal seams at this depth. A full-fold 3D survey is expected to successfully map lateral facies and thickness changes of the coal zone across the survey area.

REFLECTIVITY ANALYSIS

Vertical seismic profiles record both downgoing and upgoing wavefields, providing insight into the reflectivity of the subsurface. The ratio of incident and reflected amplitudes may be used to obtain a good estimate of the reflection coefficient of an interface, that is:

$$R_{PP} = \frac{A_{downgoing(P)}}{A_{upgoing(P)}}.$$

And for converted waves:

$$R_{PS} = \frac{A_{\text{downgoing}(P)}}{A_{\text{upgoing}(S)}},$$

where R_{PP} and R_{PS} are the reflection coefficients, and A represents the peak amplitude of a given event.

Amplitudes recorded in-situ immediately above the interface of interest are free from most wavefield propagation effects, resulting in the true amplitude reflectivity with respect to the incident wavefield. Walkaway VSP data from Red Deer were used to calculate coal reflectivity at a number of offsets, thus testing for AVO effects. The approach used was to undertake numerical modelling, followed by analysis of the field data.

Two-dimensional ray-tracing

A 1.5-dimensional model of the Cygnet strata was built using GX2 modelling software. Densities and lithologies were derived from analysis of the 9-34 well logs, whereas P- and S-wave velocities were extracted from the zero-offset mini-P and mini-S VSP surveys. Model parameters are summarized in Table 1, and the model is illustrated in Figure 10. Ray-tracing of the model was performed, using the survey geometry of the Red Deer walkaway VSP.

Table 1 Model parameters used in GX2 model of Red Deer strata.

| Layer Name | Depth to top (m) | Depth to base (m) | V_p (m/s) | V_s (m/s) | Density (kg/m^3) | V_p/V_s |
|------------|------------------|-------------------|-------------|-------------|-----------------------------|-----------|
| Layer1 | 0 | 30 | 1900 | 480 | 2321 | 3.96 |
| Layer2 | 30 | 55 | 2400 | 645 | 2365 | 3.72 |
| Layer3 | 55 | 80 | 2700 | 825 | 2418 | 3.27 |
| Layer4 | 80 | 105 | 2660 | 990 | 2422 | 2.69 |
| Layer5 | 105 | 130 | 2675 | 1180 | 2348 | 2.27 |
| Layer6 | 130 | 155 | 2700 | 1150 | 2347 | 2.35 |
| Layer7 | 155 | 180 | 2610 | 1120 | 2355 | 2.33 |
| Layer8 | 180 | 193.5 | 2825 | 1200 | 2395 | 2.35 |
| UpsandA | 193.5 | 205 | 2872 | 1500 | 2355 | 1.91 |
| LwsandA | 205 | 228 | 3080 | 1400 | 2333 | 2.2 |
| Layer9 | 228 | 230 | 3250 | 1000 | 2180 | 3.25 |
| Layer10 | 230 | 243 | 2400 | 1100 | 2342 | 2.18 |
| sandB | 243 | 251 | 3050 | 1250 | 2325 | 2.44 |
| Layer11 | 251 | 255 | 2290 | 1250 | 2408 | 1.83 |
| Layer12 | 255 | 272 | 2740 | 1300 | 2361 | 2.11 |
| SandC | 272 | 282 | 3050 | 1140 | 2427 | 2.68 |
| Ardley | 282 | 294 | 2450 | 1010 | 1905 | 2.43 |
| Layer13 | 294 | 320 | 2800 | 1300 | 2440 | 2.15 |
| Tuff | 320 | 330 | 2500 | 1100 | 2100 | 2.27 |
| Layer14 | 330 | 350 | 2800 | 1300 | 2440 | 2.15 |

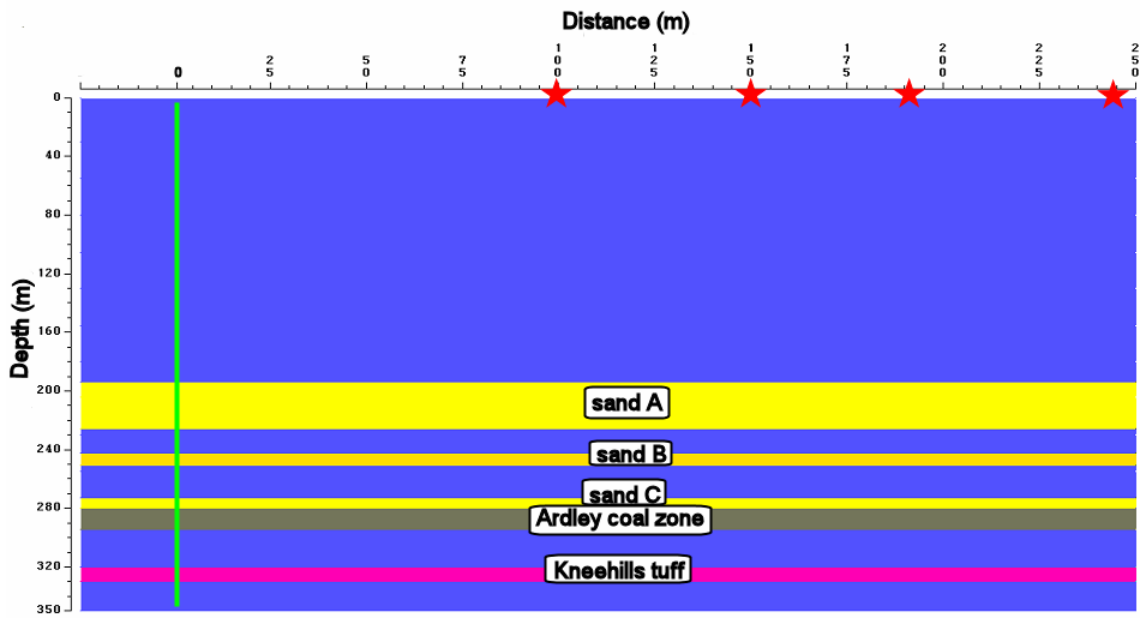


FIG. 10. Illustration of GX2 model used to numerically simulate the Red Deer study site. Sand layers are yellow, Ardley coal strata are grey, and the Kneehills tuff is pink. Wellbore is green line at distance 0, and shot points are indicated with red stars.

GX2 allows individual horizons to be turned on or off as active reflectors during raytracing. Initially, only the upper coal contact was used as an active reflector. Ray-tracing was performed in both P-P and P-S modes, and traces were generated by convolution with an 80 Hz Ricker wavelet. This wavelet was chosen to simulate the dominant frequency found in field data.

Receiver types can be varied during ray-tracing such that an omni-phone (recording the total wavefield), a vertical-component geophone, or a horizontal-component geophone may be used. Ray-tracing was run using each of these geophone types, and incidence angles were extracted from the rays in order to calculate the total wavefield amplitude from either a vertical or horizontal geophone (Figure 11).

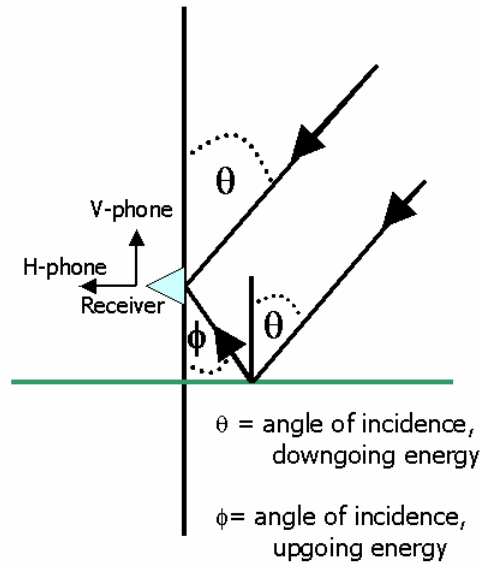


FIG. 11. Angles of incidence for downgoing and upgoing energy. Angles can be used in conjunction with vertical or horizontal amplitude to calculate the total wavefield amplitude.

Using simple triangle geometry, the amplitude of the total downgoing wavefield can be written as:

$$A_{\text{downgoing}(P)} = \frac{A_{\text{vertical}(P)}}{\cos \theta},$$

where A is the peak amplitude of a given event. In this case, amplitudes were found by examining the data in ProMAX VSP and picking the maximum (peak or trough) amplitude of the given event. The amplitude of the total upgoing wavefield can be calculated by:

$$A_{\text{upgoing}(P)} = \frac{A_{\text{vertical}(P)}}{\cos \phi}.$$

In the converted-wave case, it is easier to extract the upgoing S-wave amplitudes from the horizontal component of the receiver, so the total amplitude is found by:

$$A_{\text{upgoing}(S)} = \frac{A_{\text{horizontal}(S)}}{\sin \phi}.$$

In the GX2 model, as the reflectivity of the coal top is being examined, the only receiver made active for raytracing was that located at 279 m depth, the receiver immediately above the top of coal. Coal reflectivity was calculated using both omniphone amplitudes and those amplitudes calculated using incidence angles. The P-P reflectivity results are summarized in Table 2. Amplitudes are stated in relative values, not in units. To assess the GX2 results, reflectivities were also calculated using the CREWES Zoepritz Explorer, using incidence angles determined from the GX2 ray-tracing.

Table 2 PP reflectivity calculated using GX2 raytracing software. Reflectivity calculated using omniphone amplitudes matches that calculated using vertical-component amplitudes and angles of incidence.

| Offset (m) | Omni down amplitude | θ (degrees) | V down amplitude | Omni up amplitude | ϕ (degrees) | V up amplitude | Omni PP Reflectivity | Angled PP Reflectivity |
|------------|---------------------|--------------------|------------------|-------------------|------------------|----------------|----------------------|------------------------|
| 100 | -0.76861 | 21.607 | -0.71460 | 0.17054 | 19.222 | 0.16103 | -0.22188 | -0.22188 |
| 150 | -0.76979 | 31.135 | -0.65890 | 0.16953 | 27.919 | 0.14980 | -0.22023 | -0.22023 |
| 191 | -0.72957 | 37.674 | -0.57745 | 0.16569 | 34.027 | 0.13732 | -0.22711 | -0.22711 |
| 244 | -0.71300 | 44.672 | -0.50705 | 0.16806 | 40.737 | 0.12734 | -0.23571 | -0.23571 |

Zoeppritz equations used to calculate single-interface coal reflectivity indicate that no measurable P-P AVO gradient will be noted in the top coal reflection (Figure 12). Until large incident angles ($>50^\circ$) are reached, reflectivity varies by no more than 0.04, remaining near constant at approximately 0.22. This suggests that any amplitude variations noted in the PP reflectivities will be the result of lateral variations in coal properties, not simply an AVO effect.

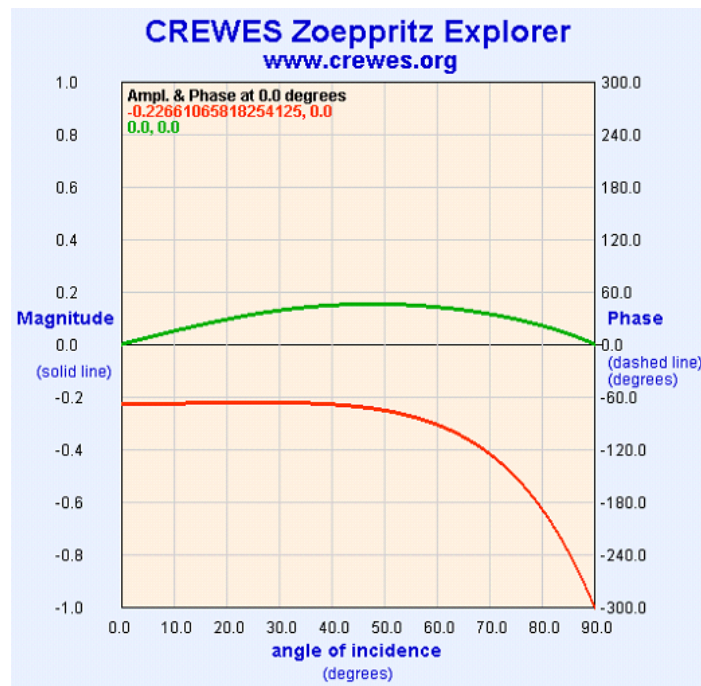


FIG. 12. Calculated Zoeppritz single-interface PP and PS reflectivity for upper coal contact using model parameters (www.crewes.org). PP reflection coefficient shows virtually no variation until incident angles of greater than about 40 degrees are reached.

Red Deer PP Reflectivity

Application of this reflection coefficient calculation technique to the Red Deer data set allows reflectivity of the Ardley coal to be evaluated. Vertical component amplitudes were used in conjunction with incident angles extracted from raytracing in order to calculate the total wavefield amplitudes, and thus, coal reflectivity. Downgoing peak

amplitudes were found using the Schlumberger separated “P-down” dataset, and upgoing amplitudes were extracted from the separated “P-up” dataset. All amplitudes were extracted from the receiver located at 279 m depth, that is, the receiver immediately above the top of the coal zone. Calculated Ardley coal zone reflectivities are summarized in Table 3. Amplitude values are digital values from processing, and are relatively scaled, not given in units.

Table 3 Summary of PP reflectivity calculated using Red Deer walkaway VSP data.

| Offset (m) | V- down amplitude | θ (degrees) | V- up amplitude | ϕ (degrees) | PP Reflectivity |
|------------|-------------------|--------------------|-----------------|------------------|-----------------|
| 100 | -43.4395 | 21.607 | 27.3347 | 19.222 | -0.61958 |
| 150 | -30.2111 | 31.135 | 22.3824 | 27.919 | -0.71767 |
| 191 | -22.7129 | 37.674 | 16.7829 | 34.027 | -0.70569 |
| 244 | -18.4502 | 44.672 | 12.5949 | 40.737 | -0.64069 |

It is immediately evident that the calculated reflectivity values from the Red Deer data set do not match those predicted by the GX2 raytracing or Zoeppritz equations. This is due to the fact that the predicted reflection coefficients are based strictly on the top of coal reflection, and do not include wavelet interference from any other reflectors. In order to more accurately predict the coal reflectivity, a detailed model of the coal was built. Blocking the well logs using a median algorithm allowed calculation of new layer parameters. Log blocks were chosen based on sharp contrasts in traveltime or density values. Original logs are shown in Figure 13, whereas blocked logs are shown in Figure 14.

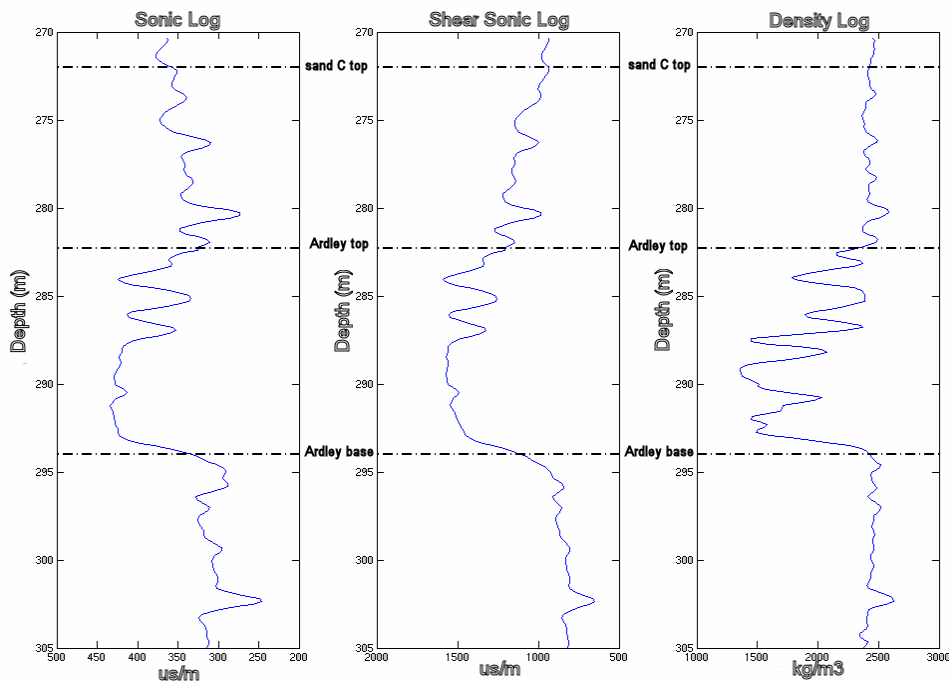


FIG. 13. Detailed well logs of the coal zone and surrounding strata, prior to blocking.

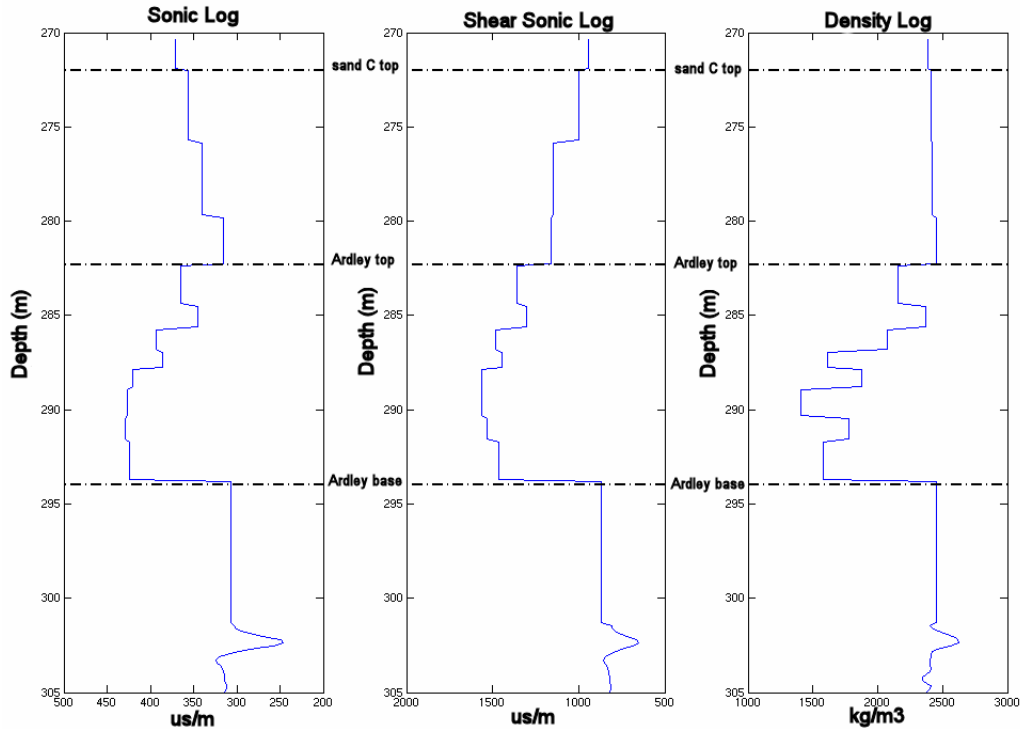


FIG. 14. Detailed well logs of coal zone and surrounding strata, after median blocking.

Amplitude analysis of results from raytracing the detailed model with all horizons turned on as active reflectors results in reflectivity values that are very close to the reflectivity calculated from the Red Deer data (Figure 15).

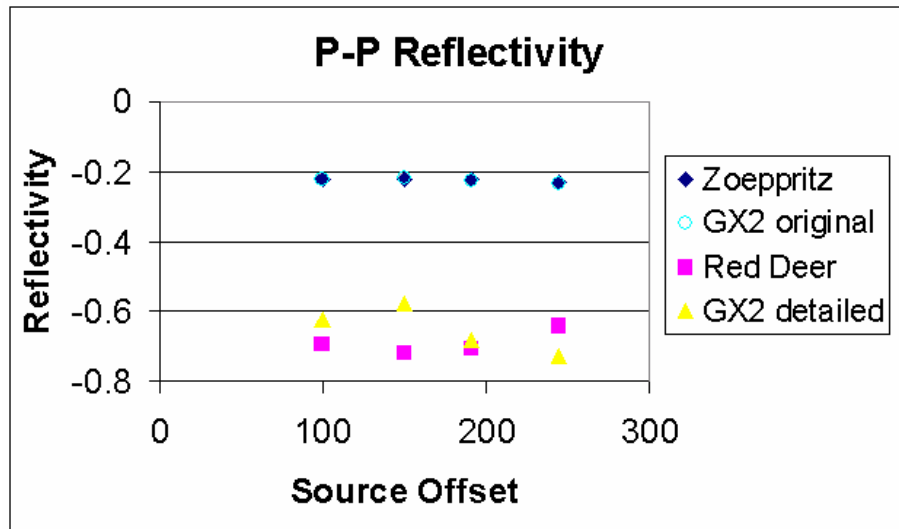


FIG. 15. Comparison of reflection coefficients derived from single interface numerical modelling, Red Deer field data, and detailed numerical modelling.

Examination of the reflectivity values from the detailed GX2 model and the Red Deer strata suggests that no measurable AVO gradient will be noted at this study site.

Although tuning effects can not be accounted for simply in Zoeppritz equations, evidence from the Red Deer data and detailed raytracing suggests that amplitude variations in coal reflections will be the result of lateral changes in thickness and/or coal properties, and not the result of AVO effects, as predicted in the simple single-layer model.

Red Deer PS Reflectivity

Zoeppritz equations used to calculate the PS reflectivity of the Red Deer coal strata indicate that a larger AVO gradient will be noted in converted-wave data than in compressional data (Figure 12). Using the same methods as those used to calculate PP reflectivity, PS reflectivity values may be calculated from the Red Deer study site. GX2 numerical modelling was performed using an 80 Hz Ricker wavelet, such that the bandwidth of the modeled converted wave matches that of the incident P-wave in the field data. In this case, downgoing P-wave amplitudes are extracted from the Schlumberger “P-down” data, whereas the upgoing S-wave amplitudes are extracted from the “S-up” data. All amplitudes were extracted from the receiver located at 279 m depth, that is, the receiver immediately above the top of the coal zone. Calculated Ardley coal zone reflectivities are summarized in Table 4. The upward angle of incidence (ϕ) for S-waves is extracted from GX2 raytracing.

Table 4 Calculated PS reflectivity values from Red Deer walkaway VSP data.

| Offset (m) | V- down amplitude | θ (degrees) | V- up amplitude | ϕ (degrees) | PS Reflectivity |
|------------|-------------------|--------------------|-----------------|------------------|-----------------|
| 100 | 97.6735 | 15.700 | -8.99687 | 11.164 | -0.08867 |
| 150 | 72.5532 | 29.396 | -10.43150 | 15.222 | -0.12526 |
| 191 | 56.3080 | 35.102 | -7.40630 | 18.238 | -0.10761 |
| 244 | 40.2603 | 44.129 | -4.53032 | 21.353 | -0.08076 |

Calculated Red Deer PS reflectivity values differ from the PS reflectivity values predicted by Zoeppritz calculations (Figure 14), although to a much lesser degree than the PP values varied. Original single-interface GX2 and Red Deer PP reflectivities differed by over 300%, whereas the maximum PS difference between single-interface modelling and field data is only 67%. Although the converted-wave data is still affected by tuning, it appears that PP reflectivity is far more influenced by tuning effects than PS data. The greater interference noted in the PP data results from the longer wavelengths present in the PP data set. In comparison, the lower PS velocities yield shorter wavelengths for the same dominant frequency, and thus, improved resolution relative to the PP data (Widess, 1973).

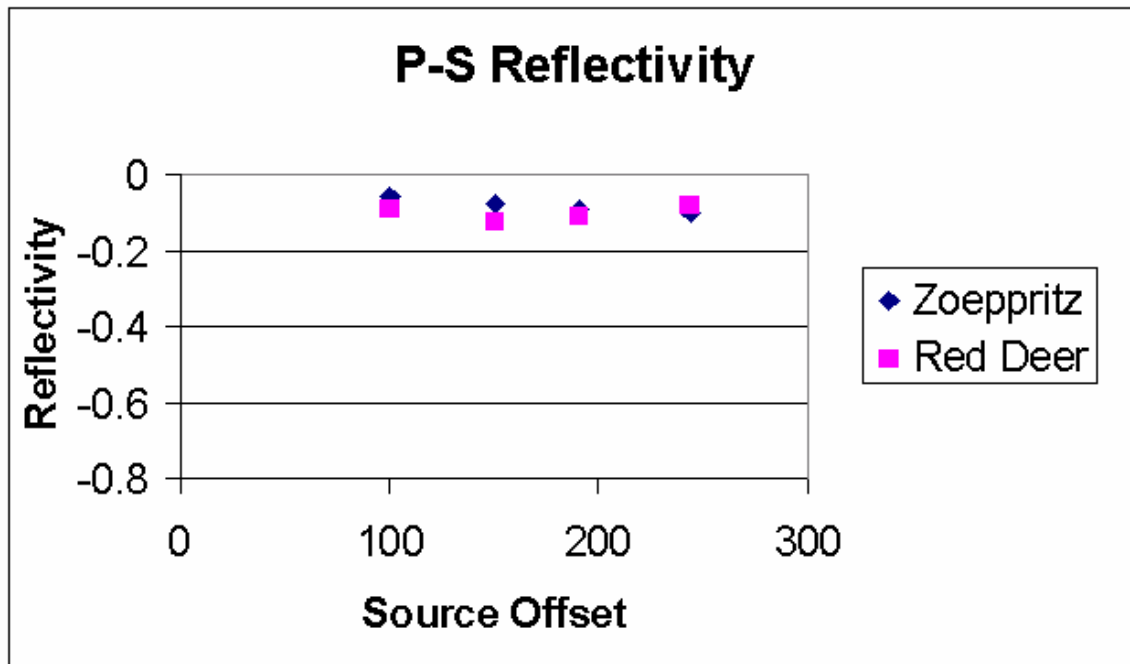


FIG. 16. Comparison of calculated Zoeppritz PS reflectivity for Ardley coal with PS reflectivity extracted from Red Deer walkaway VSP data.

As shown above, Zoeppritz calculations of expected PS reflectivity show an AVO gradient. The Red Deer reflectivity data, based on analysis of the field data, varies with offset, but not in a consistent or predictable fashion. Complexities of real data (tuning effects, noise) obscure the AVO effect predicted. It appears that large variations in PS reflectivity will, as in the PP case, most likely be a result of lateral changes in coal properties, and not simply as a function of offset.

CONCLUSIONS

Imaging of Ardley coal seams using walkaway vertical seismic profiles is effective. Both the VSP-CDP and VSP-CCP transforms (for PP and PS data, respectively) clearly image the upper and lower coal contacts. At the nearest offset (100 m), the converted-wave data was able to image an intra-coal event, unlike the PP imaging. With increasing offset, the PP data proved to be of better quality than the PS survey, and produced the better image at the farthest offset of 244 m.

Generally, the reflectivities extracted from the Red Deer data set are consistent with those predicted from known elastic properties of coal. Tuning effects are evident in the Red Deer data, resulting in much larger reflection coefficients for the top of coal than those calculated by Zoeppritz equations, particularly in the PP case. The longer wavelengths present in converted-wave data result in PS reflectivity values far less affected by tuning than PP reflectivity values, with extracted PS reflectivities much nearer those predicted theoretically.

The degree to which the PP reflectivity of the coal zone will be affected by wavelet interference will be largely dependent on both the bandwidth of the data and the number

of reflectors within the coal zone. That is, the greater the number of shale partings or tight streaks within the coal zone, the greater the effect on the PP reflectivity. As such, the difference in coal reflectivity from that predicted by Zoeppritz equations may give an indication of the vertical continuity of the coal zone, an essential factor in CBM development.

Predicted amplitude variations with offset are minimal in the PP case, and relatively minor in the PS case, suggesting that any observed amplitude variations in real coal data are the result of lateral variations in coal properties, and not simply the result of increasing incident angle. It is not possible to examine AVO in the Red Deer VSP-CDP and VSP-CCP transforms, as they display stacked amplitude variations, and are not indicative of true amplitude reflectivity. Separated raw upgoing and downgoing wavefields, however, may be used to calculate the true amplitude reflectivity of the upper coal contact. The predicted minimal AVO is borne out by the Red Deer data set, which demonstrates minor variations in extracted reflectivity, none of which are predictable based simply on offset.

REFERENCES

Widess, M.B., 1973, How thin is a thin bed? *Geophysics*, **38**, 1176-1180.

ACKNOWLEDGEMENTS

The authors gratefully acknowledge the assistance of Suncor and its partner companies, the Alberta Research Council, and Larissa Bezouchko and Mike Jones of Schlumberger. Funding for this project was received from the Alberta Energy Research Institute (AERI) and the Natural Sciences and Engineering Research Council of Canada (NSERC). We also thank the CREWES project, its sponsors, and the Alberta Ingenuity Fund for financial support.